JAMA Neurology | Original Investigation

Mapping the Supratentorial Cerebral Arterial Territories Using 1160 Large Artery Infarcts

Dong-Eog Kim, MD, PhD; Jong-Ho Park, MD, PhD; Dawid Schellingerhout, MD; Wi-Sun Ryu, MD, PhD; Su-Kyoung Lee, BS; Min Uk Jang, MD; Sang-Wuk Jeong, MD, PhD; Jeong-Yong Na, AS; Jung E. Park, MD, MS; Eun Ja Lee, MD, PhD; Ki-Hyun Cho, MD, PhD; Joon-Tae Kim, MD, PhD; Beom Joon Kim, MD; Moon-Ku Han, MD, PhD; Jun Lee, MD, PhD; Jae-Kwan Cha, MD, PhD; Dae-Hyun Kim, MD; Soo Joo Lee, MD; Youngchai Ko, MD; Byung-Chul Lee, MD, PhD; Kyung-Ho Yu, MD, PhD; Mi Sun Oh, MD, MS; Keun-Sik Hong, MD, PhD; Yong-Jin Cho, MD, PhD; Jong-Moo Park, MD, PhD; Kyusik Kang, MD; Tai Hwan Park, MD; Kyung Bok Lee, MD; Kyoung-Jong Park, PhD; Heung-Kook Choi, PhD; Juneyoung Lee, PhD; Hee-Joon Bae, MD, PhD

IMPORTANCE Cerebral vascular territories are of key clinical importance in patients with stroke, but available maps are highly variable and based on prior studies with small sample sizes.

OBJECTIVE To update and improve the state of knowledge on the supratentorial vascular supply to the brain by using the natural experiment of large artery infarcts and to map out the variable anatomy of the anterior, middle, and posterior cerebral artery (ACA, MCA, and PCA) territories.

DESIGN, SETTING, AND PARTICIPANTS In this cross-sectional study, digital maps of supratentorial infarcts were generated using diffusion-weighted magnetic resonance imaging (MRI) of 1160 patients with acute (<1-week) stroke recruited (May 2011 to February 2013) consecutively from 11 Korean stroke centers. All had supratentorial infarction associated with significant stenosis or occlusion of 1 of 3 large supratentorial cerebral arteries but with patent intracranial or extracranial carotid arteries. Data were analyzed between February 2016 and August 2017.

MAIN OUTCOMES AND MEASURES The 3 vascular territories were mapped individually by affected vessel, generating 3 data sets for which infarct frequency is defined for each voxel in the data set. By mapping these 3 vascular territories collectively, we generated data sets showing the Certainty Index (CI) to reflect the likelihood of a voxel being a member of a specific vascular territory, calculated as either ACA, MCA, or PCA infarct frequency divided by total infarct frequency in that voxel.

RESULTS Of the 1160 patients (mean [SD] age, 67.0 [13.3] years old), 623 were men (53.7%). When the cutoff CI was set as 90%, the volume of the MCA territory (approximately 54% of the supratentorial parenchymal brain volume) was about 4-fold bigger than the volumes of the ACA and PCA territories (each approximately 13%). Quantitative studies showed that the medial frontal gyrus, superior frontal gyrus, and anterior cingulate were involved mostly in ACA infarcts, whereas the middle frontal gyrus and caudate were involved mostly by MCA infarcts. The PCA infarct territory was smaller and narrower than traditionally shown. Border-zone maps could be defined by using either relative infarct frequencies or CI differences.

CONCLUSIONS AND RELEVANCE We have generated statistically rigorous maps to delineate territorial border zones and lines. The new topographic brain atlas can be used in clinical care and in research to objectively define the supratentorial arterial territories and their borders.

JAMA Neurol. 2019;76(1):72-80. doi:10.1001/jamaneurol.2018.2808
Published online September 24, 2018. Corrected on November 5, 2018.

Supplemental content

Author Affiliations: Author affiliations are listed at the end of this article.

Corresponding Author: Dong-Eog Kim, MD, PhD, Department of Neurology, Dongguk University Ilsan Hospital, 52-6 Dongguk-ro, Ilsandong-gu, Goyang-si, Gyeonggi-do 10326, Republic of Korea (kdongeog@duih.org); Hee-Joon Bae, MD, PhD, Department of Neurology, Seoul National University Bundang Hospital, 82 Gumi-ro 173 beon-gil, Bundang-gu, Seongnam, Gyeonggi-do 13620, Republic of Korea (braindoc@snu.ac.kr).

© 2018 American Medical Association. All rights reserved.

Downloaded From: https://jamanetwork.com/ on 08/27/2022

Accurate knowledge of intracranial arterial territory distribution is crucial for the radiologic assessment of infarction, which subsequently narrows or widens the scope of further investigations and ultimately guides therapeutic decision making.[1-5] However, there is much variability in published intracranial arterial territory distributions[1-16]; a seminal study by van der Zwan et al[6] investigated 50 hemispheres, demonstrating 26, 17, and 22 variations in the anterior, middle, and posterior cerebral artery (ACA, MCA, and PCA) territory, respectively. These uncertainties often confound the image-based distinction among infarcts located within an arterial territory, multiple territories, or in the border zone between arterial territories.[2,9]

There are 2 main information sources for vascular territory maps: (1) vessel injection/casting studies in anatomic specimens,[6,14-16] and (2) clinical imaging studies.[2,3,8-13] An excellent overview of vascular injection studies and microanatomical studies of cerebral blood supply by Tatu et al[1,7] produced brain maps of cerebral arterial territories depicted in graphic form applicable to clinical neuroimaging. They also provided information on the variability of the cortical territories of the 3 main cerebral arteries by defining minimal and maximal cortical areas supplied by the ACA, MCA, and PCA.

The major weaknesses of the current vascular territorial maps are (1) high variability, particularly of border zones; (2) maps were derived from only a few anatomical specimens or small sample size images and extrapolated to large populations; and (3) the specimens or images were mostly derived from younger people without ischemic disease or from people whose demographic/clinical information was not provided (eTable 1 in the Supplement). These factors make the current maps difficult to apply directly to clinical problems in an ischemic patient population.

What is needed is a modern data set that (1) can deal with variability in territories in a statistically rigorous way, (2) incorporate reasonable patient numbers, and (3) is directly applicable to the ischemic stroke patient population, in which these maps are most often clinically applied.

To address this gap in knowledge, large artery infarcts in 1160 consecutive patients were mapped to a normalized volumetric digital format. For each patient, the culprit intracranial parent vessel was clearly identifiable, allowing inferences to be drawn between the parent vessel and its vascular territory. These data are used to provide updated brain maps of the 3 main cerebral arterial territories and quantify the variability of territories and border zones, while being directly applicable to the stroke patient population.

Key Points

Question Are there ways to overcome major weakness of the current vascular territorial maps (high variability, particularly of border zones, and maps that were derived from small sample size data)?

Findings In this cross-sectional study, statistically rigorous maps were generated to delineate territorial border zones using diffusion-weighted magnetic resonance imaging of 1160 consecutive patients with acute supratentorial infarction owing to atherosclerotic intracranial large artery steno-occlusion. Border zones could be defined using either relative infarct frequencies or the Certainty Index that reflects the likelihood of a voxel being a member of a specific vascular territory.

Meaning This new topographic brain atlas can be used to objectively define the supratentorial arterial territories and their borders.

Methods

This is a multicenter study that involved 11 academic stroke centers in Korea. From May 2011 to February 2013, we consecutively enrolled 1160 patients (eFigure in the Supplement) with acute ischemic stroke within 7 days after symptom onset who had diffusion-weighed magnetic resonance imaging (DWI MRI)–confirmed supratentorial large artery atherosclerosis (LAA) infarction owing to significant (>50%) stenosis or occlusion of a single large cerebral artery (in the absence of significant proximal stenosis or occlusion of the intracranial and extracranial carotid arteries) on MR angiography, computed tomography (CT) angiography, or conventional angiography: ACA (n = 71), MCA (n = 896), or PCA (n = 193). The institutional review boards of all participating centers approved this study. All patients or their legally authorized representatives provided written informed consent.

We mapped the 3 vascular territories individually to a standardized volumetric template, generating 3 data sets showing the frequency of infarct for each voxel by affected parent vessel. These data sets were merged to create a set of volumetric figures. We then mapped the 3 vascular territories collectively, generating a data set of Certainty Index (CI) maps to show in each voxel the fraction of ACA-, MCA-, or PCA-related infarcts as a fraction of the total large territory infarct incidence (defined as the sum of the 3 territory frequencies). We performed quantification studies, including volume (percentage) measurements of infarcts and the vascular territories and region-of-interest (ROI)–based analyses, to calculate mean CIs for a territory (vs the others) in selected cortical gyri and white matter areas.

MRI and Lesion Registration for Brain Mapping

Brain imaging was performed on 1.5-T (n = 995) or 3.0-T (n = 165) MRI systems. All scans were transferred to the Korean Brain MRI Data Center for central data storage and quantitative analysis. As previously reported,[17-19] high-signal intensity lesions on DWIs were segmented and registered onto the Montreal Neurological Institute template. The registered binary images for acute infarcts in the ACA, MCA, and PCA group of patients were used to generate voxel-based lesion frequency maps and CI maps, with vascular territories encoded by color on the maps.

Vascular Territory Mapping

A first set of lesion frequency maps was generated to display the lesion frequency in each voxel by calculating the frequencies of that voxel being involved in ACA, MCA, and PCA infarcts and by coding 3 different colors (green, red, and blue, respectively) with varying brightness levels for each color: a brighter color for a higher frequency (heatmaps). Color blending was performed for interterritorial overlap areas. The

© 2018 American Medical Association. All rights reserved.

Downloaded From: https://jamanetwork.com/ on 08/27/2022

frequency maps for each infarct category were then merged to create a set of figures.

A second set of frequency heatmaps without overlap areas was generated by modifying the first set of maps by (1) comparing the ACA/MCA/PCA lesion frequencies in each voxel of the inter-territorial areas and (2) allocating the voxel as the territory of a cerebral artery associated with the highest infarct frequency on the voxel. The few voxels with equal frequencies were not color-coded.

Then, CI maps were generated to reflect the likelihood of a voxel being a member of a vascular territory vs the other territories: ie, 3 CIs (for ACA/MCA/PCA infarction) at each voxel. Briefly, for each vascular territory, the infarct frequency at each voxel was divided by total frequency (sum of ACA, MCA, and PCA) for that voxel to yield a fraction, the CI. A relatively high CI for 1 vascular territory (vs 2 CIs for the other vascular territories) at a voxel indicates that most of the infarcts at that voxel are caused preferably by the territorial parent artery, suggesting definite membership in the vascular territory. A relatively low CI indicates that infarcts at that voxel location could be caused by another territorial parent vessel. Similar levels of CIs indicate that the voxel is likely located in a border zone between territories.

Next, we wanted to explore the border zones between the vascular territories and created maps to this end. For each voxel found to have nonzero frequencies of infarction, we tested for equality or near equality among the lesion frequencies of pairings of ACA, MCA, and PCA. We empirically defined near equality as a frequency difference (ie, the difference between overlapping territorial values) of each voxel not to exceed 10% of the highest value of infarct frequencies in every supratentorial voxel for all vascular territories. For the ACA-MCA pairing, a voxel was colored yellow if the condition of equality or near equality was met; for the MCA-PCA pair, the voxel was colored purple; and for the ACA-PCA pair, blue. All other voxels were left uncolored in these maps to highlight the border zones between vascular territories.

Finally, interterritory line maps based on CI differences were generated to elucidate the divisions between territories more precisely. Where vascular territorial overlap (ACA-MCA, MCA-PCA, or ACA-PCA) showed near equal frequencies (see previous paragraph), we calculated the difference between 1 CI at the voxel for 1 vascular territory and the other CI for the paired vascular territory at that voxel. The absolute value of the CI difference was color-coded to represent the relative likelihood of that voxel being a member of the vascular territory with the higher CI: green, red, and blue for the ACA-dominant, MCA-dominant, and PCA-dominant border zone, respectively. In other words, we forced a choice (based on CI differences) within the known border-zone areas, causing a sharp change of color, or line, to appear, indicating where the probabilities of infarct changed from 1 parent vessel to the next. This technique accentuates small differences and forces the larger and more vague zones to show as much sharper lines of division, facilitating visualization and description, although at the expense of probably excessive precision in the territorial border lines so defined.

Qualitative and Quantitative Studies

After qualitative comparisons of vascular territories on the Tatu et al atlas[7] and our atlas by visual inspection, we performed quantitative analyses using our map data. Moreover, for easier interpretation of lesion distribution in each vascular territory, we generated additional maps (**Figure 1**) showing the anatomical information (with abbreviations), which was derived from the Automated Anatomical Atlas.[20]

Statistical Analysis

SPSS, version 18.0 (IBM) was used to perform either *t* test or analysis of variance for continuous variables, and χ^2 test for categorical variables. Two-sided *P* values less than .05 were considered significant.

Results

Figures 2, **3**, and **4** show the supratentorial vascular territorial maps generated using the DWI data of 1160 patients with acute stroke (mean [SD] age, 67.0 [13.3] years; 623 men) with supratentorial infarction and significant stenosis or occlusion of the ACA, MCA, or PCA (**Table**). Roman numerals are used for the section numbers of the Tatu et al maps,[7] whereas arabic numerals are used for those of the maps from this study. Numbers that range from 13 to 24 were chosen to retain consistency with those in the Tatu et al atlas[7] (XIII-XXIV for the supratentorial region of the brain; Figure 1).

Visual inspection of frequency maps (Figure 2) and MCA-CI maps (Figure 3A) indicated that the borders of the MCA territory generally extended anteriorly to superior frontal sulcus, and posteriorly to middle occipital gyrus (sections 16-21). Superiorly (sections 22-24), there was anterior involvement of middle frontal gyrus and posterior involvement of parietal lobule and angular gyrus. Inferiorly (sections 13-15), there was anterior involvement of inferior frontal gyrus and middle frontal gyrus. Posteriorly, the MCA territory could extend to inferior occipital gyrus and middle occipital gyrus. The MCA area involved the putamen in the sections 14 to 16, the globus pallidus in the sections 15 to 17, and the insula in the sections 14 to 18.

The PCA territory included the interhemispheric surfaces of the occipital lobes (lingual gyrus, calcarine gyrus, and lower half of cuneus), the thalami, and midbrain (sections 13-19; Figures 2 and 3B). The lateral border of the PCA territory was located lateral to frontal gyrus (section 13), extending posteriorly to inferior occipital gyrus (sections 13-14), and middle occipital gyrus (sections 16-17), and superior occipital sulcus (sections 18-19).

The ACA territory (Figures 2 and 3C) included medial frontal gyrus and superior frontal gyrus (sections 19-24), and anterior and middle parts of the cingulate (sections 15-22) and corpus callosum (sections 16-20). Moreover, the ACA territory extended posteriorly to precuneus (sections 20-24) and splenium (sections 19-20). Infarcts were infrequently observed in the orbitofrontal regions (sections 13-14) and frontal tips (sections 15-18), which are regarded to be the ACA territory.

The most medial point for the MCA territory was the caudate. The most anterior point for the PCA territory was the an-

© 2018 American Medical Association. All rights reserved.

Downloaded From: https://jamanetwork.com/ on 08/27/2022

Figure 1. Anatomy Atlas

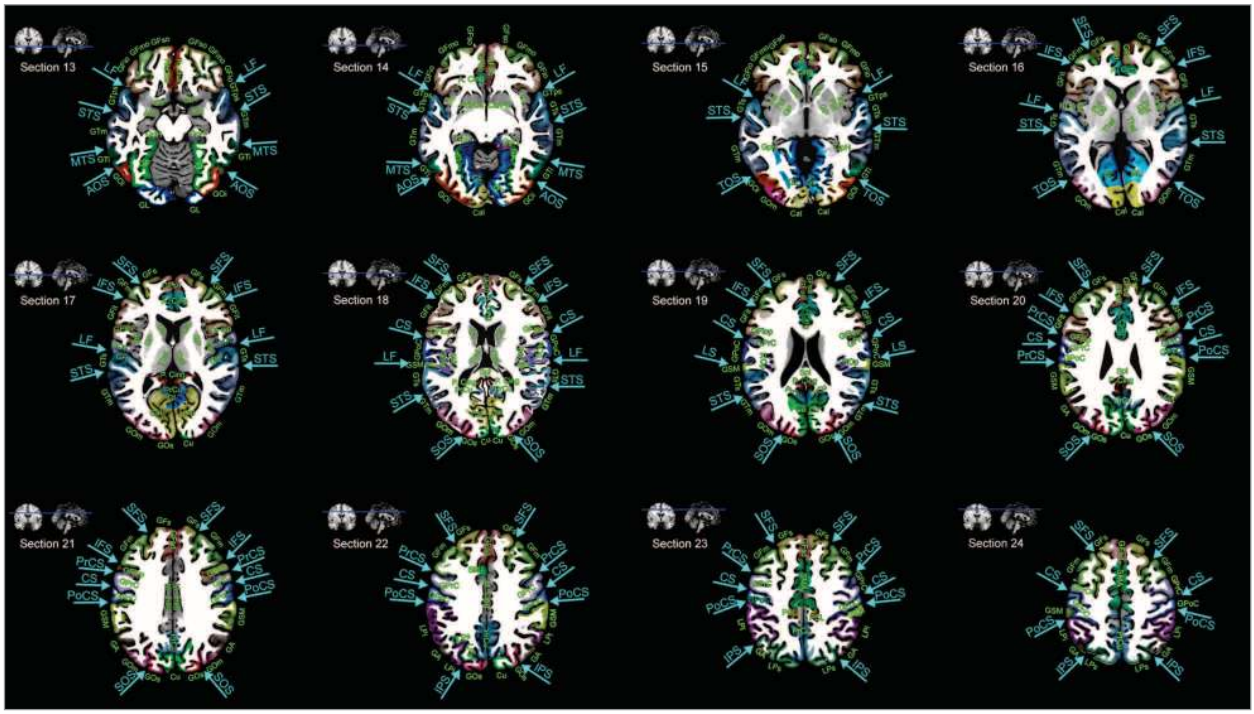

The Montreal Neurological Institute ch2better-templates and the Automated Anatomical Atlas[20] were used to display anatomic information in the supratentorial brain: z = −14.5 mm (section 13), −8.5 mm (section 14), −2.5 mm (section 15), 3.5 mm (section 16), 9.5 mm (section 17), 15.5 mm (section 18), 21.5 mm (section 19), 27.5 mm (section 20), 33.5 mm (section 21), 39.5 mm (section 22), 45.5 mm (section 23) mm, and 51.5 mm (section 24) superior to the reference axial plane: anterior commissure–posterior commissure plane. A. Cing indicates anterior cingulate gyrus; GA, angular gyrus; Cal, calcarine gyrus; Cu, cuneus; GF, fusiform gyrus; GFd, medial frontal gyrus; GFdo, orbital part of the medial frontal gyrus; GFsd, superior part of the medial frontal gyrus; GFi, inferior frontal gyrus; GFio, orbital part of the inferior frontal gyrus; GFiop, opercular part; GFit, triangularis; GFm, middle frontal gyrus; GFmo, orbital part of the middle frontal gyrus; GFs, superior frontal gyrus; GFso, orbital part of the superior frontal gyrus; GH, Heschl gyrus; GpH, parahippocampal gyrus; GL, lingual gyrus; GOi, inferior occipital gyrus; GOm, middle occipital gyrus; GOs, superior occipital gyrus; GPoC, postcentral gyrus; GPrC, precentral gyrus; GSM, supramarginal gyrus; GTs, superior temporal gyrus; GTps, temporal pole; GTi, inferior temporal gyrus; GTm, middle temporal gyrus; LPi, inferior parietal lobule; LPs, superior parietal lobule; M. Cing, middle cingulate gyrus; Olf, olfactory gyrus; P. Cing, posterior cingulate gyrus; PCL, paracentral lobule; PrCu, precuneus; Rectus, gyrus rectus; Rop, rolandic operculum; AOS, anterior occipital sulcus; CS, central sulcus; IFS, inferior frontal sulcus; IPS, intraparietal sulcus; LF, lateral fissure; MTS, middle temporal sulcus; PrCS, precentral sulcus; PoCS, postcentral sulcus; SFS, superior frontal sulcus; STS, superior temporal sulcus; TOS, temporooccipital sulcus; Am, amygdala; Ca, caudate; GP, globus pallidus; Ins, Insula; Put, putamen; SMA, supplementary motor area; SOS, superior occipital sulcus; Spl, splenium; Thal, thalamus.

terior thalamus. The entire interhemispheric sulcus was shared between the ACA and PCA.

Anterior cerebral artery-MCA borders in our maps largely agreed with those in the Tatu et al maps[7] (Figures 2 and 4). However, MCA-PCA borders in our maps (inferior occipital gyrus or middle occipital gyrus) lay medial to those in the Tatu et al maps (middle temporal gyrus), suggesting that the PCA territory may be narrower than previously known. The width of overlapping border zones reflecting the territorial variability (Figure 4A) was relatively narrow in the anterosuperior boundary (yellow areas) of the MCA territory compared with the posteroinferior boundary (purple areas).

Certainty Index map-based quantitative analysis (eResults and eTable 2 in the Supplement) of anterior brain areas showed that medial frontal gyrus, superior frontal gyrus, and anterior cingulate gyrus were involved mostly by ACA infarcts, whereas middle frontal gyrus and caudate were involved mostly by MCA infarcts. In posterior brain areas, PCA infarct territory, located in lower and middle brain regions, was narrower than on currently available maps, and infarct territories in upper brain regions had a complex z-axis dependency.

Mean (SD) infarct volumes (percent per total supratentorial brain parenchyma) in the ACA, MCA, and PCA groups were respectively 0.65% (0.74%), 1.39% (2.44%), and 0.67% (1.11%). In the CI maps, the mean ACA, MCA, and PCA territorial volume percent per total supratentorial brain parenchyma were respectively 13.3%, 54.1%, and 13.8%, when a "display cutoff CI" for each territory was set as 90%. Undetermined regional volume was 20.2% (eTable 3 in the Supplement).

Discussion

This multicenter study on cerebrovascular topography is unique because, to our knowledge, it has the largest sample size ever (eTable 1 in the Supplement) and provides not only lesion frequency maps but also CI maps with probabilistic estimation of vascular territories and borders. These maps

© 2018 American Medical Association. All rights reserved.

Downloaded From: https://jamanetwork.com/ on 08/27/2022

Figure 2. Infarct Frequency Maps With or Without Interterritorial Overlaps Displayed as Color Blends

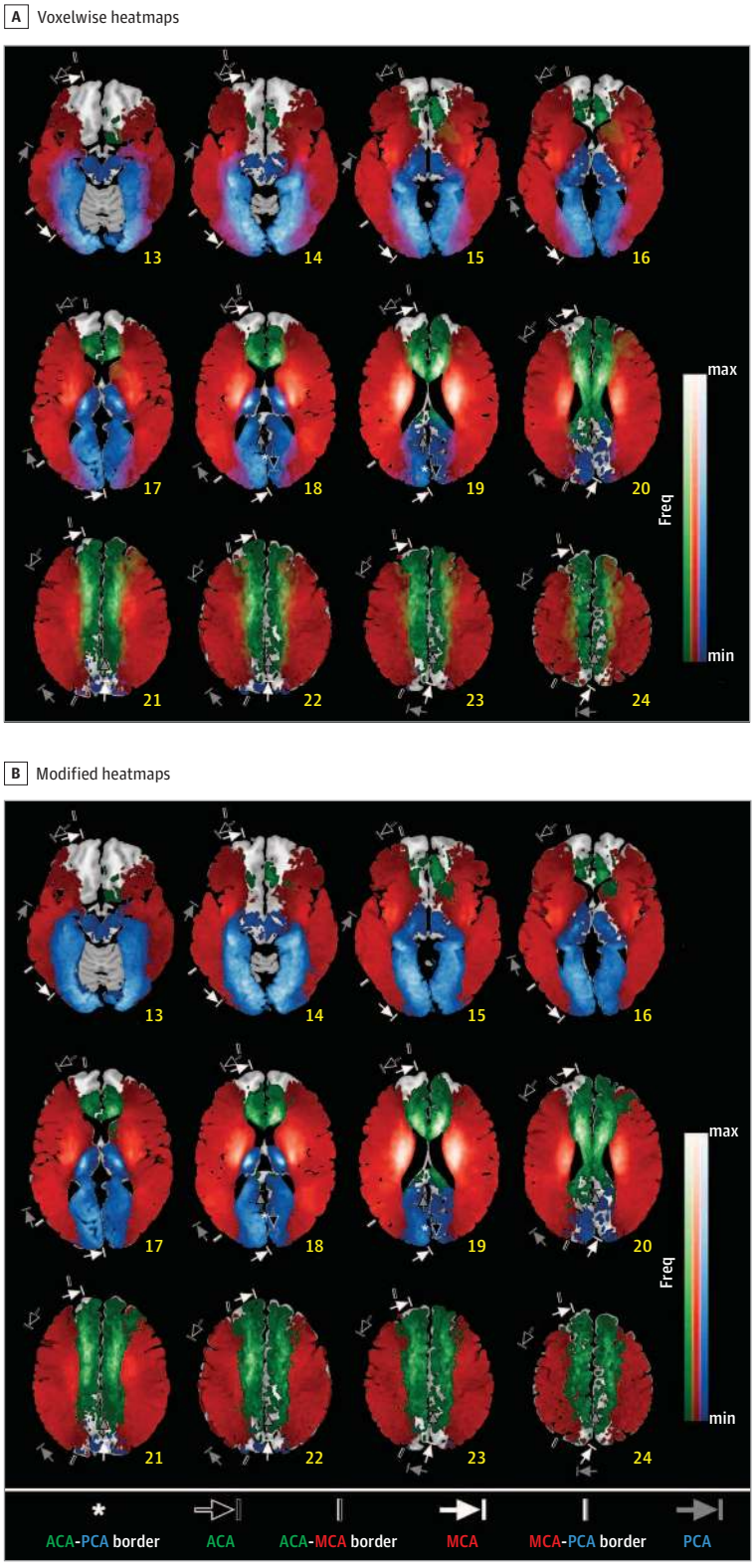

A, Voxelwise lesion frequency heatmaps were generated using diffusion-weighted magnetic resonance imaging data of patients with acute ischemic stroke admitted with anterior/middle/posterior cerebral artery (ACA, MCA, and PCA) infarction associated with significant stenosis or occlusion of a relevant large artery (N = 1160). Maximum (max) frequencies are 23.9% (17 of 71) for the ACA (green), 14.6% (131 of 896) for the MCA (red), and 17.6% (34 of 193) for the PCA (blue). Color blending was performed for interterritorial overlap areas. Annotations show territorial variabilities that are noted in the Tatu et al atlas.[7] B, Figure 2A was modified by allocating each voxel in the overlapping areas as the territory of a cerebral artery associated with the highest infarct frequency on the voxel. The few voxels with equal or near equal frequencies were not color-coded. Maximum (max) frequencies are 23.9% (17 of 71) for the ACA (green), 14.6% (131 of 896) for the MCA (red), and 17.6% (34 of 193) for the PCA (blue). Annotations show territorial variabilities that are noted in the Tatu et al atlas.[7] The right hemispheric brain mapping is depicted on the left side of the figure. Freq indicates frequency; min, minimum.

showed that medial frontal gyrus, superior frontal gyrus, and anterior cingulate gyrus were involved mostly by ACA infarcts, whereas middle frontal gyrus and caudate were involved mostly by MCA infarcts. It was notable that PCA in-

© 2018 American Medical Association. All rights reserved.

Downloaded From: https://jamanetwork.com/ on 08/27/2022

farct territory was narrower than expected. Infarct territories in the upper posterior brain regions changed complexly with (z-axis-dependent) order. When the cutoff CI was set as 90%, the MCA territorial volume (approximately 54% of the total supratentorial volume) was about 4-fold bigger than the ACA and PCA volumes, both of which were similar (approximately 13% of the total supratentorial volume). The remaining undetermined region was about 20%, which includes not only border zones but also the areas where infarcts were infrequently observed, such as orbitofrontal regions and frontal tips, both of which are known to be the ACA territory.

It has been argued that most currently available maps are difficult to interpret because of a limited number of brain sections represented and variable territorial boundaries noted. Contrary to Duret's description in 1874[14] and prevailing knowledge of vascular territory as shown in standard textbooks, numerous morphological or functional studies showed the presence of interindividual variation in the distribution of cerebral arteries.[2,3,6,9-11,13]

To circumvent these constraints, the Tatu et al atlas[7] displays the maximum and minimum territories of each vascular territory.[1] However, the wide variability displayed on the atlas often restricts reliable determination of infarct territories, thus complicating the assessment of stroke mechanism and the choice of drugs to prevent recurrent stroke. According to the Tatu et al atlas,[1] infarcts in middle temporal gyrus and middle occipital gyrus (section XIX) probably belong to 2 different vascular territories, ie, MCA and PCA, respectively. However, the atlas also informs that the lesions could belong to a single vascular territory, ie, the MCA territory. Our study (eTable 2 in the Supplement) demonstrates that the mean CIs for middle temporal gyrus infarcts and middle occipital gyrus infarcts in the equivalent section to be the MCA territory are 91.7% and 82.3%, respectively, (vs 0% and 6.4% for those infarcts to be the ACA territory), greatly favoring a single territorial stroke vs a dual territorial stroke. With this probabilistic information as well as in the absence of cardioembolic source of cerebral infarction, clinicians would feel more confident with prescribing antiplatelet drugs for secondary prevention.

Tatu et al[7] reported that the cortical branches of the MCA most commonly supply the area on the lateral surface of the hemisphere extending to superior frontal solcus, intraparietal sulcus, and inferior temporal gyrus. On the orbitofrontal surface, the MCA territory on their maps included the lateral orbital gyrus, which is a part of inferior frontal gyrus. Our study confirmed these findings. In addition, our maps showed that inferior temporal gyrus and inferior occipital gyrus could be involved by both MCA infarcts and PCA infarcts, although inferior occipital gyrus was involved mostly by MCA lesions. Tatu et al[7] explained that the maximum MCA area could cover the entire lateral surface of the hemisphere.[7] However, the MCA area in our study did not reach the interhemispheric fissure.

Tatu et al[7] described that the cortical branches of the ACA most commonly supply the medial surface of the hemisphere extending into superior frontal sulcus and the parietooccipital sulcus. They also noted that the cortical ACA territory supplied inferior frontal sulcus. With relation to the orbitofrontal cortex, the ACA territory on their map included the medial orbital gyrus. Our study showed that inferior frontal sul-

Figure 3. Certainty Index (CI) Maps

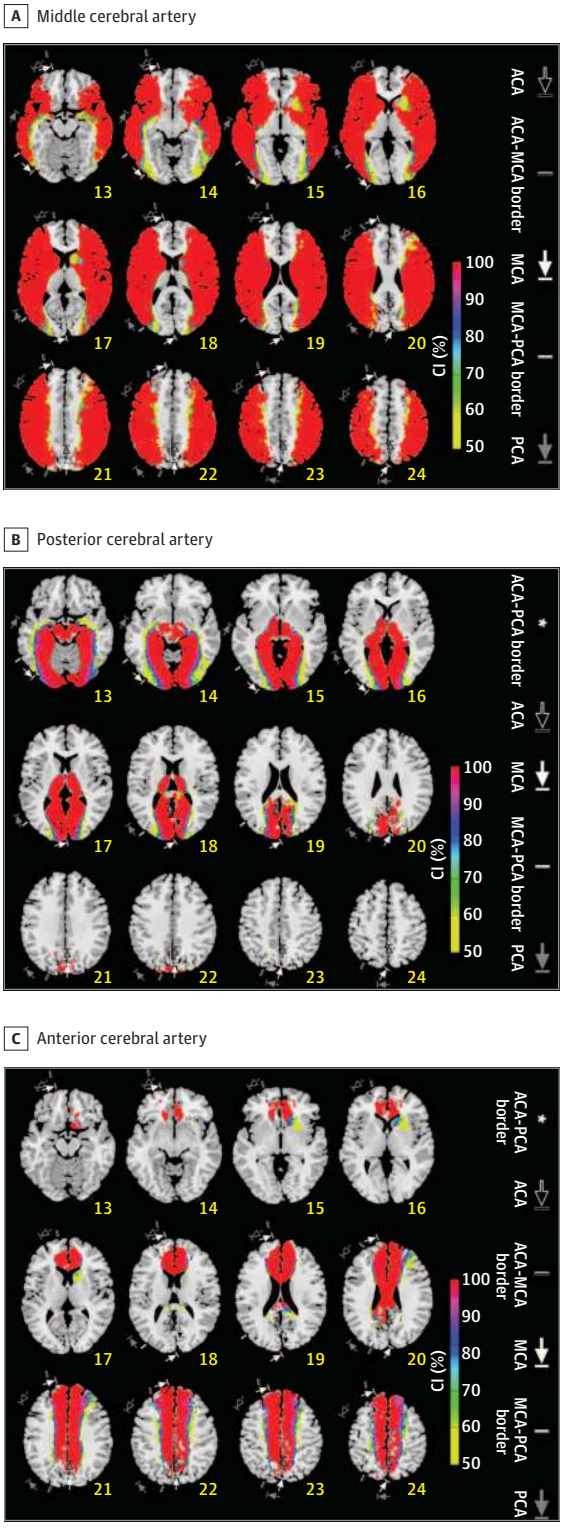

A-C, CI maps for the middle/posterior/anterior cerebral artery (MCA/ACA/PCA, respectively). CI reflects the likelihood of a voxel being a member of a specific vascular territory vs the other territories: either ACA, MCA, or PCA infarct frequency divided by total infarct frequency in each voxel. Annotations show territorial variabilities that are noted in the Tatu et al atlas.[7] Right hemispheric brain mapping is depicted on the left side.

© 2018 American Medical Association. All rights reserved.

Downloaded From: https://jamanetwork.com/ on 08/27/2022

Figure 4. Interterritorial Border Zone Maps and Line Maps

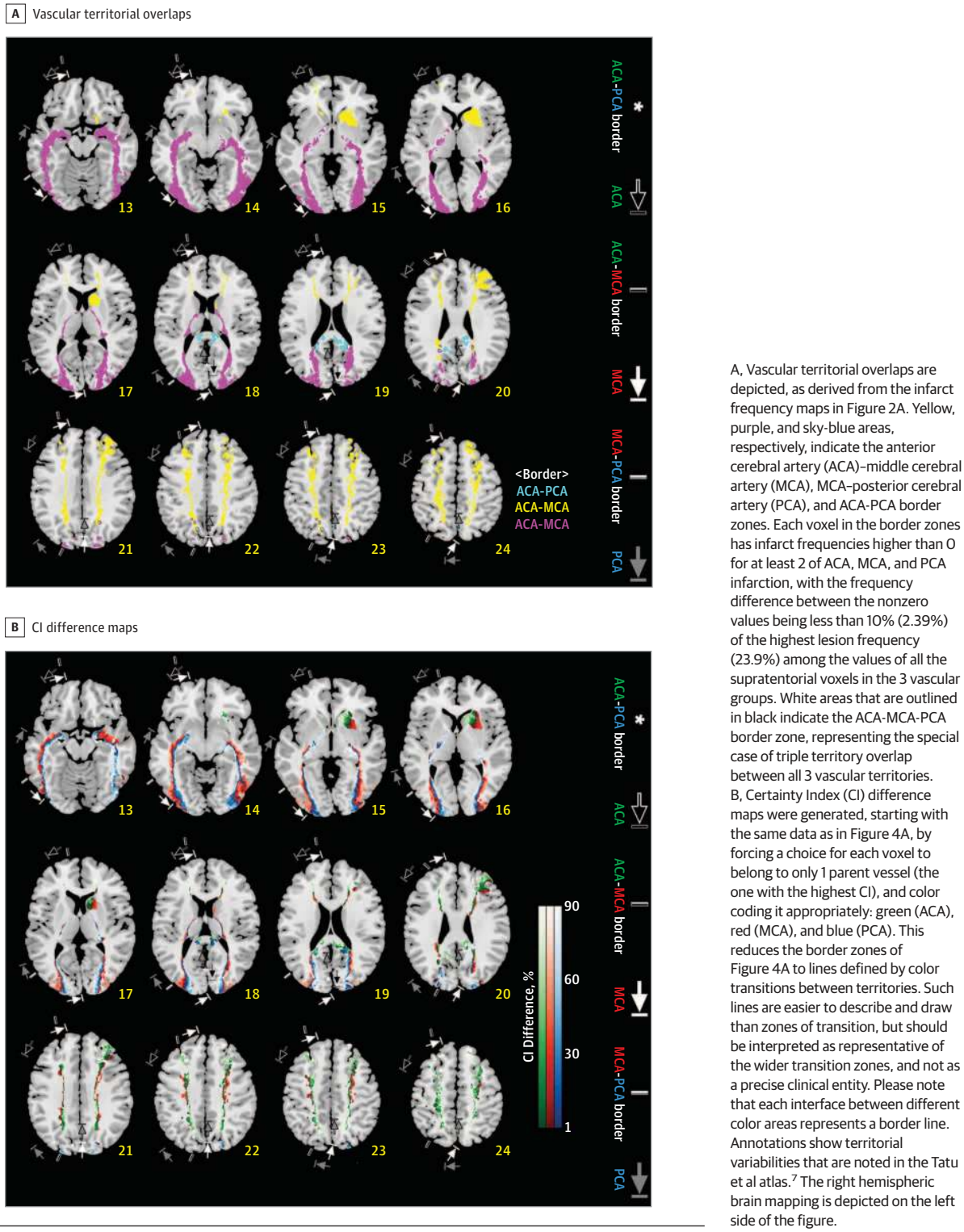

A, Vascular territorial overlaps are depicted, as derived from the infarct frequency maps in Figure 2A. Yellow, purple, and sky-blue areas, respectively, indicate the anterior cerebral artery (ACA)–middle cerebral artery (MCA), MCA–posterior cerebral artery (PCA), and ACA-PCA border zones. Each voxel in the border zones has infarct frequencies higher than 0 for at least 2 of ACA, MCA, and PCA infarction, with the frequency difference between the nonzero values being less than 10% (2.39%) of the highest lesion frequency (23.9%) among the values of all the supratentorial voxels in the 3 vascular groups. White areas that are outlined in black indicate the ACA-MCA-PCA border zone, representing the special case of triple territory overlap between all 3 vascular territories. B, Certainty Index (CI) difference maps were generated, starting with the same data as in Figure 4A, by forcing a choice for each voxel to belong to only 1 parent vessel (the one with the highest CI), and color coding it appropriately: green (ACA), red (MCA), and blue (PCA). This reduces the border zones of Figure 4A to lines defined by color transitions between territories. Such lines are easier to describe and draw than zones of transition, but should be interpreted as representative of the wider transition zones, and not as a precise clinical entity. Please note that each interface between different color areas represents a border line. Annotations show territorial variabilities that are noted in the Tatu et al atlas.[7] The right hemispheric brain mapping is depicted on the left side of the figure.

cus involved MCA infarcts, and the upper portion of posterior cingulate gyrus, which is in front of the parieto-occipital sulcus, involved mostly ACA infarcts, whereas the lower portion mostly involved PCA infarcts. In addition, the orbitofrontal cortex was rarely affected by cerebral infarction.

Phan et al[2] reported on a digital atlas showing the probability of involvement of MCA infarction at each voxel. The T2-weighted MRI from 28 patients with infarcts in the right hemisphere were flipped along the y-axis, allowing for all infarcts to lie on the unilateral (left hemispheric) side of the image, thereby

© 2018 American Medical Association. All rights reserved.

Downloaded From: https://jamanetwork.com/ on 08/27/2022

Table. Demographic Data for the Study Population

Parameter	No. (%)				P Value[a]
	Total (n = 1160)	ACA (n = 71)	MCA (n = 896)	PCA (n = 193)	
Age, y, mean (SD)	67.0 (13.3)	71.1 (11.6)	66.6 (13.7)	67.6 (12.1)	.02
Male	623 (53.7)	23 (32.4)	477 (53.2)	123 (63.7)	<.01
Hypertension	774 (66.7)	54 (76.1)	601 (67.1)	119 (61.7)	.08
Diabetes	374 (32.2)	25 (35)	278 (31.0)	71 (36.8)	.26
Hyperlipidemia	401 (34.6)	19 (26.8)	322 (35.9)	60 (31.1)	.16
Smoking	468 (40.3)	15 (21.1)	380 (42.4)	73 (37.8)	<.01
Coronary artery disease	62 (5.3)	2 (2.8)	49 (5.5)	11 (5.7)	.62
Atrial fibrillation	0	0	0	0	NA
Prior use of statin	173 (14.9)	6 (8.5)	142 (15.8)	25 (13.0)	.17
Previous use of antiplatelet	264 (22.8)	13 (18.3)	204 (22.8)	47 (24.4)	.58
Thrombolysis (intravenous or intraarterial)	184 (15.9)	6 (8.5)	161 (18.0)	17 (8.8)	<.01
NIHSS score, mean (SD)	6.1 (5.5)	4.7 (4.0)	6.6 (5.6)	4.5 (4.8)	<.01
Last known normal time to imaging, h, mean (SD)	37.9 (45.6)	43.8 (43.4)	37.5 (46.6)	37.8 (41.9)	.54

Abbreviations: ACA, anterior cerebral artery; MCA, middle cerebral artery; NA, not applicable, NIHSS, National Institute of Health Stroke Scale; PCA, posterior cerebral artery.

[a] Intergroup differences were assessed using analysis of variance for continuous variables. The χ^2 test was used for categorical variables.

doubling the sample size. Moreover, their probabilistic maps for the MCA territory were not adjusted for the other 2 main cerebral arteries (ie, ACA and PCA) that supply the adjacent territories while probably competing with the MCA in the border zone.

We investigated the topography of the 3 cerebral arteries collectively (a data set of 3-group CI maps) as well as individually (3 data sets of frequency maps) using nonflipped DWIs from a substantially larger number (n = 1160) of consecutive patients with acute LAA infarction in 1 of the ACA, MCA, or PCA territories. Our study largely confirms 3-dimensional MCA boundaries described by Phan et al[2] but at a much higher resolution. Moreover, unlike in their study, superior frontal gyrus in the upper half of the supratentorial brain was involved mostly by ACA infarcts and infrequently by MCA infarcts in our maps. This is also in discordance with the report of Tatu et al,[7] which showed that the MCA branches supply the superior frontal gyrus, and the PCA branches supply the inferomedial surfaces of the temporal and occipital lobes extending to the parieto-occipital sulcus. They also explained that the PCA area could extend as far as to superior temporal sulcus and the upper part of the precentral sulcus.[7] Our study results, on the other hand, showed that the extent of the affected PCA area was relatively small, without extending to superior temporal sulcus or precentral sulcus.

It is difficult to determine the location of cortical border zones between the ACA, MCA, and PCA because of individual differences in the territories supplied by the major arteries, the development of leptomeningeal collaterals, and the anatomy of cerebral cortex.[21] In our maps, border zones are represented as overlapping lesion areas with relative lesion frequencies or CI differences displayed. The comprehensive data sets likely enable clinicians and researchers to define border zones in a customized way. The posterior border zone between the MCA and PCA areas lies mostly in middle occipital gyrus, not in middle temporal gyrus as noted in the Tatu et al atlas.[7] This finding, as well as the MCA-PCA borderline shown in the interterritory line maps based on CI differences, again demonstrates that the extent of the PCA area may be narrower than previously thought.

Limitations

A notable difficulty in studying vascular supply territories is introduced by variations of the circle of Willis anatomy. For example, in the presence of the fetal-type PCA that originates from the distal portion of the internal carotid artery, thromboembolism from the more proximal portion of the ipsilateral internal carotid artery could result in PCA territory infarction as well as MCA or ACA territory infarction. We excluded patients with significant proximal stenosis or occlusion of the ipsilesional intracranial and extracranial carotid arteries (that might give rise to ACA vs MCA ambiguity in the infarct attribution). However, some patients with significant stenosis or occlusion of the MCA or ACA could have seemingly pure anterior circulation infarcts but actually mixed anterior and posterior circulation infarcts if (1) ipsilateral fetal-type PCA is present and (2) culprit plaques are in the proximal carotid arteries despite a mild degree of stenosis (ie, <50% stenosis). Such cases might have contributed to the finding that the PCA territory looked narrower than previously known; particularly in the PCA-CI maps rather than in the PCA infarct frequency maps, because the CI was calculated in the same manner as for positive predictive value, which is influenced by the prevalence of disease (ie, voxelwise frequency of PCA infarcts vs all infarcts). Thus, further studies are required to account for the variations of the circle of Willis anatomy in the topographic mapping. What is also needed is research on territorial mapping of deep brain infarcts owing to nonsuperficial arteries (eg, tuberothalamic artery and anterior choroidal artery) as well as of infratentorial infarcts.

Conclusions

We have generated a high-resolution digital atlas of supratentorial infarction using DWIs of 1160 patients with acute LAA stroke. Despite limitations, the topographic atlas and quantitative data (eTable 2 in the Supplement) can be used to objectively define the supratentorial arterial territories and the interterritorial border using predetermined threshold criteria on the lesion frequencies or CIs.

© 2018 American Medical Association. All rights reserved.

Downloaded From: https://jamanetwork.com/ on 08/27/2022

ARTICLE INFORMATION

Accepted for Publication: July 6, 2018.

Correction: This article was corrected on November 5, 2018, to correct errors to the Corresponding Author section and to correct Dr Jong-Ho Park's affiliation.

Published Online: September 24, 2018. doi:10.1001/jamaneurol.2018.2808

Author Affiliations: Department of Neurology, Dongguk University College of Medicine, Dongguk University Ilsan Hospital, Goyang, Korea (D.-E. Kim, Ryu, S.-K. Lee, Jeong, Na, J. E. Park); Korean Brain MRI Data Center, Dongguk University Ilsan Hospital, Goyang, Korea (D.-E. Kim, Ryu, S.-K. Lee, Jeong, Na, J. E. Park); Department of Neurology, Myongji Hospital Hanyang University College of Medicine, Goyang, Korea (J.-H. Park); Department of Radiology, The University of Texas MD Anderson Cancer Center, Houston (Schellingerhout); Department of Cancer Systems Imaging, The University of Texas MD Anderson Cancer Center, Houston (Schellingerhout); Department of Neurology, Dongtan Sacred Heart Hospital, Hwaseong, Korea (Jang); Department of Radiology, Dongguk University Ilsan Hospital, Goyang, Korea (E. J. Lee); Department of Neurology, Chonnam National University Hospital, Gwangju, Korea (K.-H. Cho, J.-T. Kim); Department of Neurology, Seoul National University College of Medicine, Seoul National University Bundang Hospital, Seongnam, Korea (B. J. Kim, Han, Bae); Department of Neurology, Yeungnam University Hospital, Daegu, Korea (J. Lee); Department of Neurology, Dong-A University Hospital, Busan, Korea (Cha, D.-H. Kim); Department of Neurology, Eulji University Hospital, Daejeon, Korea (S. J. Lee, Ko); Department of Neurology, Hallym University Sacred Heart Hospital, Anyang, Korea (B.-C. Lee, Yu, Oh); Department of Neurology, Ilsan Paik Hospital, Inje University, Goyang, Korea (Hong, Y.-J. Cho); Department of Neurology, Nowon Eulji Medical Center, Eulji University, Seoul, Korea (J.-M. Park, Kang); Department of Neurology, Seoul Medical Center, Seoul, Korea (T. H. Park); Department of Neurology, Soonchunhyang University Hospital, Bucheon, Korea (K. B. Lee); Daium Inc, Busan, Korea (K.-J. Park); Department of Computer Science, Inje University, Gimhae, Korea (Choi); Department of Biostatistics, Korea University College of Medicine, Seoul, Korea (J. Lee).

Author Contributions: Dr Dong-Eog Kim had full access to all of the data in the study and takes responsibility for the integrity of the data and the accuracy of the data analysis.
Concept and design: D.-E. Kim, J.-H. Park, Schellingerhout, Jeong, E. J. Lee, Han, Jun Lee, Y.-J. Cho, K.-J. Park, Bae.
Acquisition, analysis, or interpretation of data: D.-E. Kim, Schellingerhout, Ryu, S.-K. Lee, Jang, Jeong, Na, J.-E. Park, K.-H. Cho, J.-T. Kim, B. J. Kim, Cha, D.-H. Kim, S. J. Lee, Ko, B.-C. Lee, Yu, Oh, Hong,
Y.-J. Cho, J.-M. Park, Kang, T. H. Park, K. B. Lee, Choi, Juneyoung Lee, Bae.
Drafting of the manuscript: D.-E. Kim, J.-H. Park, Schellingerhout, Han, Cha, J.-M. Park, K.-J. Park.
Critical revision of the manuscript for important intellectual content: D.-E. Kim, J.-H. Park, Schellingerhout, Ryu, S.-K. Lee, Jang, Jeong, Na, J. E. Park, E. J. Lee, K.-H. Cho, J.-T. Kim, B. J. Kim, Jun Lee, D.-H. Kim, S. J. Lee, Ko, B.-C. Lee, Yu, Oh, Hong, Y.-J. Cho, Kang, T. H. Park, K. B. Lee, Choi, Juneyoung Lee, Bae.
Statistical analysis: D.-E. Kim, K.-J. Park, Juneyoung Lee.
Obtained funding: D.-E. Kim, Bae.
Administrative, technical, or material support: D.-E. Kim, J.-H. Park, Ryu, Jang, Na, Han, D.-H. Kim, S. J. Lee, Oh, Hong, J.-M. Park, K. B. Lee, Choi, Bae.
Supervision: D.-E. Kim, Schellingerhout, Jeong, J. E. Park, K.-H. Cho, B. J. Kim, B.-C. Lee, Y.-J. Cho, Bae.

Conflict of Interest Disclosures: None reported.

Funding/Support: This study was supported by grants from National Center for Standard Reference Data, Korean Agency for Technology and Standards, Ministry of Trade, Industry and Energy, Ministry of Health and Welfare (grant HI12C1847; Korea Healthcare Technology R&D Project), and Global Research Lab program (grant NRF-2015K1A1A2028228) of the National Research Foundation, funded by the Korean government, Republic of Korea.

Role of the Funder/Sponsor: National Center for Standard Reference Data and Korean Agency for Technology and Standards have helped the Korean Brain MRI Data Center with establishing traceability and managing uncertainty of quantitative magnetic resonance imaging measurements. Otherwise, funders did not have a role in the design and conduct of the study; collection, management analysis, and interpretation of the data; preparation, review, or approval of the manuscript; and decision to submit the manuscript for publication.

Additional Contributions: We thank Sun-Young Chung, BS, Yu-Hwa Kim, Jung-Ok Nam, BS, Eun-Hee Park, and Min-Kyung Yang, BS, for helping quantitative image registration, and Mi Hwa Yang, MS, Myung Suk Jang, AS, MiHoon Jang, AS, and Min-Ji Choi, BS, for the collection of large-scale imaging data. They received financial compensation from funding sponsors for these works.

REFERENCES

1. Tatu L, Moulin T, Bogousslavsky J, Duvernoy H. Arterial territories of the human brain: cerebral hemispheres. *Neurology*. 1998;50(6):1699-1708. doi:10.1212/WNL.50.6.1699

2. Phan TG, Donnan GA, Wright PM, Reutens DC. A digital map of middle cerebral artery infarcts associated with middle cerebral artery trunk and branch occlusion. *Stroke*. 2005;36(5):986-991. doi:10.1161/01.STR.0000163087.66828.e9

3. Berman SA, Hayman LA, Hinck VC. Correlation of CT cerebral vascular territories with function, I: anterior cerebral artery. *AJR Am J Roentgenol*. 1980;135(2):253-257. doi:10.2214/ajr.135.2.253

4. Hayman LA, Berman SA, Hinck VC. Correlation of CT cerebral vascular territories with function, II: posterior cerebral artery. *AJR Am J Roentgenol*. 1981;137(1):13-19. doi:10.2214/ajr.137.1.13

5. Berman SA, Hayman LA, Hinck VC. Correlation of CT cerebral vascular territories with function, 3: middle cerebral artery. *AJR Am J Roentgenol*. 1984;142(5):1035-1040. doi:10.2214/ajr.142.5.1035

6. van der Zwan A, Hillen B, Tulleken CA, Dujovny M, Dragovic L. Variability of the territories of the major cerebral arteries. *J Neurosurg*. 1992;77(6):927-940. doi:10.3171/jns.1992.77.6.0927

7. Tatu L, Moulin T, Vuillier F, Bogousslavsky J. Arterial territories of the human brain. *Front Neurol Neurosci*. 2012;30:99-110. doi:10.1159/000333602

8. Damasio H. A computed tomographic guide to the identification of cerebral vascular territories. *Arch Neurol*. 1983;40(3):138-142. doi:10.1001/archneur.1983.04050030032005

9. Hennerici M, Daffertshofer M, Jakobs L. Failure to identify cerebral infarct mechanisms from topography of vascular territory lesions. *AJNR Am J Neuroradiol*. 1998;19(6):1067-1074.

10. Takahashi S, Suzuki M, Matsumoto K, et al. Extent and location of cerebral infarcts on multiplanar MR images: correlation with distribution of perforating arteries on cerebral angiograms and on cadaveric microangiograms. *AJR Am J Roentgenol*. 1994;163(5):1215-1222. doi:10.2214/ajr.163.5.7976904

11. Kim SJ, Kim IJ, Kim YK, et al. Probabilistic anatomic mapping of cerebral blood flow distribution of the middle cerebral artery. *J Nucl Med*. 2008;49(1):39-43. doi:10.2967/jnumed.107.045724

12. Taoka T, Iwasaki S, Nakagawa H, et al. Distinguishing between anterior cerebral artery and middle cerebral artery perfusion by color-coded perfusion direction mapping with arterial spin labeling. *AJNR Am J Neuroradiol*. 2004;25(2):248-251.

13. van Laar PJ, Hendrikse J, Golay X, Lu H, van Osch MJ, van der Grond J. In vivo flow territory mapping of major brain feeding arteries. *Neuroimage*. 2006;29(1):136-144. doi:10.1016/j.neuroimage.2005.07.011

14. Duret H. Recherches anatomiques sur la circulation de l'encephale. *Arch Physiol Norm Pathol*. 1874;60:316-353.

15. Heubner O. *Die luetischen Erkrankungen der Himarterien*. Leipzig, Germany: FCW Vogcl Verlag; 1874:170-214.

16. Beevor CE. On the distribution of the different arteries supplying the human brain. *Philos Trans R Soc Lond*. 1909;200:1-55. doi:10.1098/rstb.1909.0001

17. Kim DE, Park KJ, Schellingerhout D, et al. A new image-based stroke registry containing quantitative magnetic resonance imaging data. *Cerebrovasc Dis*. 2011;32(6):567-576. doi:10.1159/000331934

18. Ryu WS, Woo SH, Schellingerhout D, et al. Grading and interpretation of white matter hyperintensities using statistical maps. *Stroke*. 2014;45(12):3567-3575. doi:10.1161/STROKEAHA.114.006662

19. Ryu WS, Woo SH, Schellingerhout D, et al. Stroke outcomes are worse with larger leukoaraiosis volumes. *Brain*. 2017;140(1):158-170. doi:10.1093/brain/aww259

20. Lancaster JL, Woldorff MG, Parsons LM, et al. Automated Talairach atlas labels for functional brain mapping. *Hum Brain Mapp*. 2000;10(3):120-131. doi:10.1002/1097-0193(200007)10:3<120::AID-HBM30>3.0.CO;2-8

21. Mangla R, Kolar B, Almast J, Ekholm SE. Border zone infarcts: pathophysiologic and imaging characteristics. *Radiographics*. 2011;31(5):1201-1214. doi:10.1148/rg.315105014

© 2018 American Medical Association. All rights reserved.

Downloaded From: https://jamanetwork.com/ on 08/27/2022